CO_2-Laser-Metal Coupling in Vacuum

A. M. Bouveret*
Office National d'Etudes et de Recherches Aérospatiales, Châtillon, France

Pulsed CO_2-laser energy coupling experiments to duraluminum in vacuum are reported. At high fluence (>75 J/cm^2) the heat coupling coefficient value is found close to 0.3, more than expected at low pressure. Moreover, bulk vaporization and breakdown appear in isolated sites. The high infrared absorptivity drop of the metal during melting and spatial overintensities due to the presence of surface defects could explain these findings.

Nomenclature

A_S, A_T	= area of the laser spot and target surface, respectively
C_p	= specific heat
d_{air}	= air layer thickness
d_{DS}	= flake or surface defect thickness
E_0	= incident pulse energy
F_0	= incident fluence
F_{DS}, I_{DS}	= fluence and intensity thresholds for the surface defect vaporization, respectively
I_0	= laser incident intensity
I_c	= breakdown threshold
k_{air}	= thermal conductivity of the air
L_f, L_v	= melting and vaporization heats, respectively
m	= mass of the sample
m_f, m_v	= ejected liquid and vapor masses, respectively
p_0	= air ambient pressure
T_0	= ambient temperature
T_{f_1}, T_{f_2}, T_v	= solids, liquid, vaporization temperatures, respectively
ΔT	= mean temperature increase of the sample
$\alpha, \bar{\alpha}$	= absorptivity and mean absorptivity on a temperature range, respectively
α_t	= thermal coupling coefficient
α_T	= total energy transfer coefficient
α_v	= enthalpic coupling coefficient
ΔT	= mean temperature increase of the sample
ρ	= volumic mass
τ	= pulse length
τ_c	= breakdown delay
τ_{peak}	= spike-peak time
τ_q	= spike length
τ_{f_1}	= melting delay
τ_v	= vaporization delay

I. Introduction

THE thermal coupling on metal targets by pulsed CO_2 laser at ambient atmospheric pressure has recently been the object of much research and is well understood today. It has been shown that at $I_0 < I_c$, the metal surface behaves as an efficient infrared reflector with a thermal coupling coefficient $\alpha_t < 0.1$. When $I_0 > I_c$, an ambient air plasma ignited by the surface defects of the target induces an absorption wave whose strength and velocity increase with the incident intensity. The plasma induced by the breakdown and the absorption wave radiates primarily in the ultraviolet and visible wavelength ranges; these radiations are mostly absorbed by the metal surface, and α_t increases sharply near the breakdown threshold. With incident intensities close to I_c, α_t was found to be about 0.35 for aluminum. Nevertheless, for $I_0 > I_c$, α_t decreases as I_0 increases because, at atmospheric pressure, the higher the absorption front velocity, the weaker the target-plasma coupling. For high I_0 values, α_t values are so low that the surface melting is obtained with difficulty.

By contrast at low pressures, the absorption wave becomes faint. As a result, α_t values should be close to the infrared intrinsic absorptivity of the material. In fact, preceding experiments show that:

1) A breakdown occurs and induces high α_t values; on steel,[3] $\alpha_t = 0.20$ at $p_0 = 10^{-1}$ Torr; on aluminum alloy,[4] $\alpha_t = 0.14$ at $p_0 = 4.10^{-2}$ Torr; on pure aluminum,[2] $\alpha_t = 0.20$ at $p_0 = 0.5$ Torr.

2) The breakdown occurs in the metal vapor.[4]

3) The plasma remains confined to the plasma spot,[4] thus inducing a strong beam-target coupling.

Accordingly, the following question is raised: Is it possible to find α_t values close to 0.35 in vacuum as at $p_0 = 760$ Torr? In this paper, we present experiments on duraluminum, carried out at a small value of A_S/A_T as in Ref. 2, showing that such energy coupling values can be found at high fluences, when the breakdown occurs early in the pulse. In such conditions a crater appears, and it is necessary to introduce an "enthalpic" coupling coefficient, defined by Eq. (2); α_v differs from α_T, the total energy transfer coefficient, by the fraction of energy transformed into kinetic energy of the ejected liquid and vapor masses.

The experimental setup and experiments are described in Sec. II; a one-dimensional nonlinear heating code that provides the values of τ_{f_1} and τ_v is described in Sec. III, and the experimental results are both given and interpreted in Sec. IV.

II. Experimental Setup and Experiments

The pulsed CO_2 electron-beam laser was built at ONERA. It delivers a pulse of energy $E_0 = 10$ J; the time shape of the pulse, smoothed for a later numerical use, is given in Fig. 1: $\tau = 20$ μs, $\tau_q = 0.26$ μs, $\tau_{peak} = 0.13$ μs.

The time dependence of the incident intensity (Fig. 1) was measured by a photon-drag detector. The square section laser beam was focused on an area of 3.06 mm^2, small enough to produce a rapid vaporization. The spatial profile of the beam was determined from the prints on a plexiglass sheet. The spot homogeneity was evaluated in the same way; local overintensities of 40% were detected. Lower values of the pulse energy were obtained by a set of attenuators and measured for each shot by a calibrated calorimeter.

The targets used to measure α_t were 1-mm thick duraluminum disks, mechanically polished and cleaned with

Presented as Paper 83-1441 at the AIAA 18th Thermophysics Conference, Montreal, Canada, June 1-3, 1983; received Nov. 23, 1983; revision received Oct. 22, 1984.

*Research Engineer, Thermophysics Division.

alcohol before each experiment. A 100-μm diameter chromel-alumel thermocouple was embedded into the rear surface of the sample, at the center.

Experiments at constant intensity and decreasing pressure were carried out in order to determine the pressure threshold p_{cr}, below which the absorption wave in residual air becomes faint and is replaced by a luminous, underexpanded, supersonic vapor free-jet: on the one hand, α_t tends to become constant for p_0 decreasing under p_{cr}; on the other hand, the characteristic shapes of both luminous phenomena differ strongly so that open-shutter views enables them to be distinguished. These experiments, not detailed here, gave $p_{cr} \approx 0.1$ Torr.

Thus, the coupling experiments were carried out at $p_0 = 4.10^{-2}$ Torr, which can be considered as vacuum. Experiments consisted of recording the following observations, at pulse space-time shape and varying E_0:

α_t is deduced from

$$\alpha_t = mC_p\Delta T/E_0 \tag{1}$$

where ΔT is measured by a thermocouple.

α_v is calculated from

$$\alpha_v = \alpha_t + (m_f\Delta H_f + m_v\Delta H_v)/E_0 \tag{2}$$

where

$$\Delta H_f = L_f + \int_{T_0}^{T_m} C_p \mathrm{d}T, \quad \Delta H_v = L_f + L_v + \int_{T_0}^{T_v} C_p \mathrm{d}T$$

are evaluated numerically and m_f and m_v are measured.

In the present case, α_v was evaluated, assuming that the removed mass $\Delta m = m_f + m_v$ was wholly transformed into vapor: $m_f = 0$; this hypothesis is reasonable because the liquid layer is very thin (maximum thickness, given by a numerical code: 2μm) and the part of the liquid not transformed into vapor resolidifies at the crater edge (Fig. 7a). The Δm value, about 0.1 mg, was measured by a microbalance as the difference between the sample masses before and after irradiation; it was also estimated by measuring the crater size with a profilometer, as follows:

1) An open-shutter profile photo of the surface was taken during each shot in order to detect the existence and the shape and size of the plasma.

2) An impact enlargement was made after each shot in order to analyze the target damage.

The tests were carried out for several target diameters (15, 10, 5 mm) to evaluate the effect of the plasma radiation on the value of α_t, the "size effect." For the target diameter 5 mm, the values of the ratio A_S/A_T in the present experiments and those of Ref. 2 are close, and the results can be compared.

III. Numerical Code of Surface Heating

In order to explain the experiments, the melting and vaporization delays τ_{fl} and τ_v, the surface heating until vaporization are estimated computationally in terms of E_0. The breakdown is usually assumed to occur just after the vaporization; thus $\tau_c \approx \tau_v$.

Two kinds of vaporization are usually considered in the literature:

1) A uniform surface vaporization, the bulk vaporization.

2) A weak vaporization of thermally insulated surface defects[1,5] occurring much earlier than bulk vaporization, eventually followed by a weak breakdown.

Thermally Insulated Defect Model

The vaporization model for air-layer thermally insulated surface defects used to explain the low threshold ignition on metal surface at normal pressure[1,5] is applied here at low pressure.

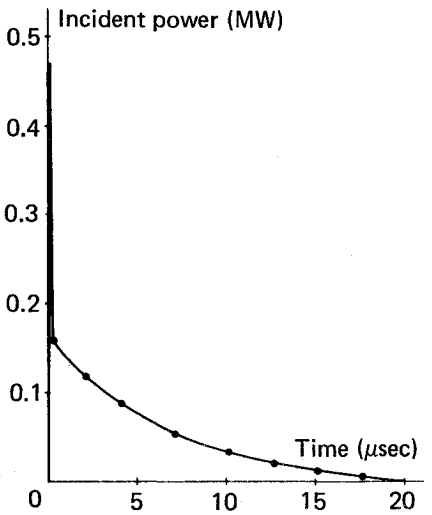

Fig. 1 Incident laser power time variation for $E_0 = 1$ J. Smoothed experimental data.

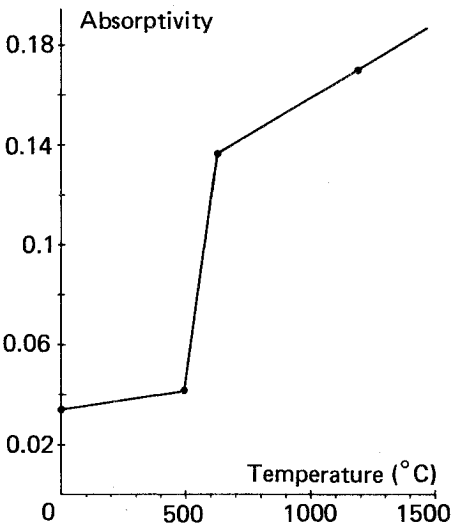

Fig. 2 Temperature dependence of duraluminum absorptivity; experimental data.[6]

Surface defects assumed to be 0.2-μm thick lamellas, thermally insulated from the surface by an 1-μm thick air-layer, are vaporized when the following thresholds are reached:

$$I_{DS} = k_{air}(T_v - T_0)/(d_{air}\tilde{\alpha}) \tag{3}$$

$$F_{DS} = \rho C_p d_{DS}(T_v - T_0)/\tilde{\alpha} \tag{4}$$

At $p_0 = 4.10^{-2}$ Torr, a numerical application to the duraluminum, with $\tilde{\alpha} = 0.09$, gives: $F_{DS} = 0.8$ J/cm^2 and $I_{DS} = 0.4$ MW/cm^2. These values are reached in the pulse spike (Fig. 1) for $E_0 > 0.7$ J.

Uniform Surface Heating Model

For a 1.75-mm squre spot and $t < \tau = 20$ μs, the maximal heated depth value is about 0.05 mm and the heating calculation can be done in one dimension. A nonlinear finite difference method is used, taking into account the pulse shape and the temperature dependence of the absorptivity and the thermal properties. Figure 2 gives the experimental temperature dependence of the absorptivity,[6] obtained with a 400-W cw laser. For duraluminum, without thermodynamic data, the vapor-pressure relation is assumed to be similar to that of pure aluminum:

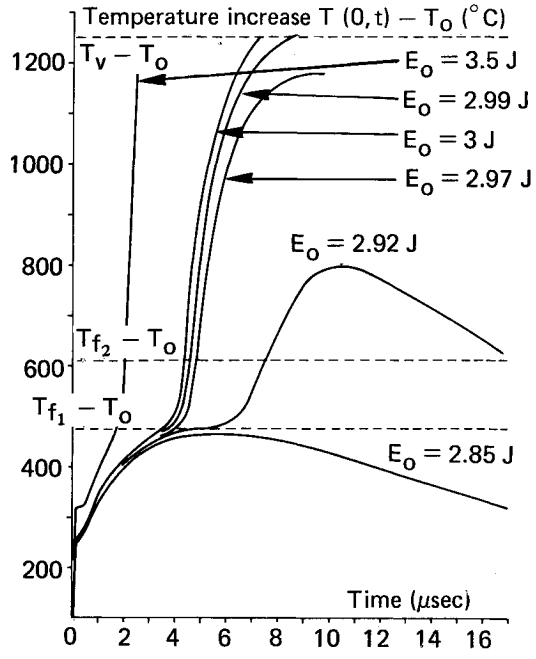

Fig. 3 Time variation of the front-surface temperature increase at the energy E_0; numerical results; $T_0 = 27°C$.

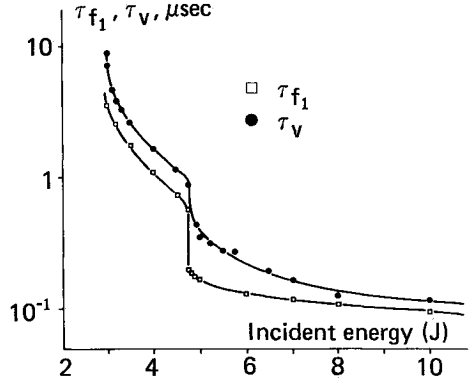

Fig. 4 Melting and vaporization delays vs incident energy E_0; numerical results.

$$T_v(p_0) = \frac{35300}{\ell n(3.9 \times 10^5 / p_0)} \qquad (5)$$

where p_0 is an atmospheres and T_v in degrees Kelvin.

Figure 3 shows that melting and vaporization occur at $E_0 = 2.90$ J ($F_0 = 95$ J/cm^2) and 2.98 J ($F_0 = 97.5$ J/cm^2), respectively, i.e., at very close energy and fluence thresholds; this fact comes from the sharp absorptivity drop during the melting. The fluence range between melting and vaporization thresholds is very narrow. Thus, in these experiments, there is a low probability for melting to occur alone. As a rule, if a surface point melts, it vaporizes a few microseconds later. The isolated craters shown in Fig. 6b could follow from this phenomenon, the hot points coming from the presence of surface defects inducing strong local overintensities.

For 2.90 J $< E_0 <$ 2.98 J or $95 < F_0 < 97.5$ J/cm^2, after melting, the surface remains liquid without vaporizing during the last part of the pulse, about 15 μs; during this period, the absorptivity is high and a sharp α_t increase is expected.

For $E_0 > 2.98$ J, a part of absorbed energy is released through vaporization; as the $\tau_v - \tau_{f_1}$ delay decreases sharply from 5 μs for $E_0 = 2.98$ J to 0.8 μs for $E_0 = 3.5$ J (Fig. 4), α_t must bend down, as observed experimentally (Fig. 5).

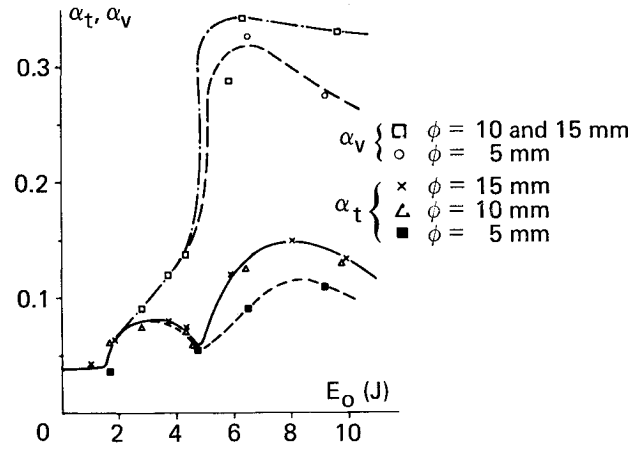

Fig. 5 Thermal and enthalpic coupling coefficients α_t, α_v vs incident energy E_0. Target size effect. Experimental results for the duraluminum at $p_0 = 4.10^{-2}$ Torr.

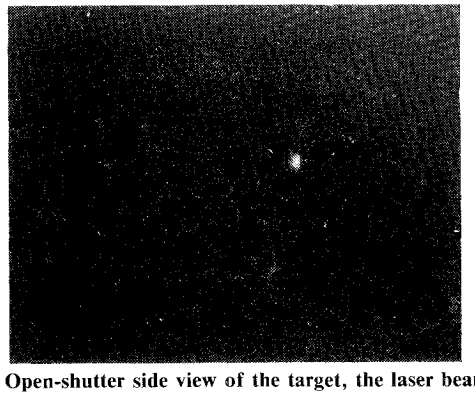

Fig. 6a Open-shutter side view of the target, the laser beam comes from left; $E_0 = 2.75$ J; plasma diameter: 7 mm.

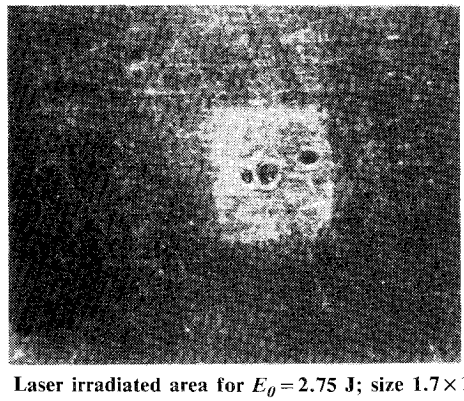

Fig. 6b Laser irradiated area for $E_0 = 2.75$ J; size 1.7×1.8 mm^2.

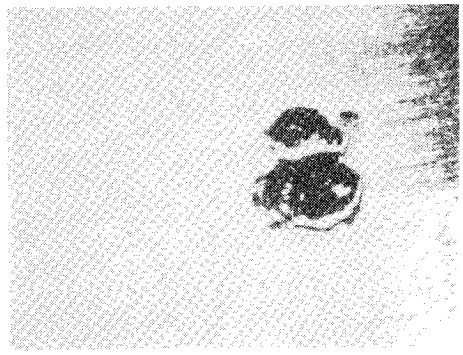

Fig. 6c Laser irradiated area for $E_0 = 4.35$ J.

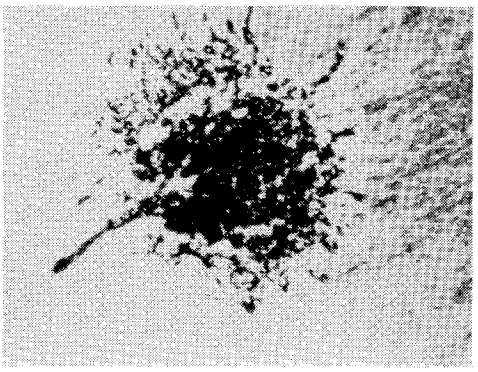

Fig. 7a Laser irradiated area for $E_0 = 6.4$ J.

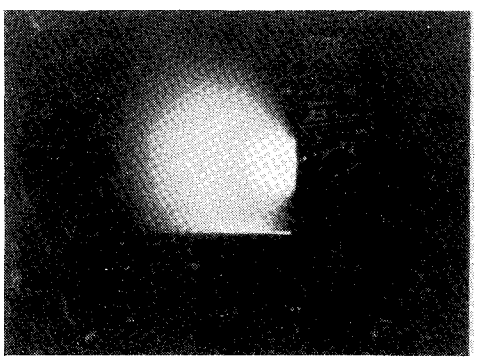

Fig. 7b. Open-shutter side view of the target for $E_0 = 6.4$ J. Same scale as Fig. 6a.

IV. Observations and Interpretation

The $\alpha_t(E_0)$ plot (Fig. 5) shows several significant energy ranges, interpreted by the numerical code described above:

$E_0 < 1.5$ J

The surface is not altered as observed at magnification 14×, there is no plasma, and $\alpha_t = 0.04$, corresponding to low temperature intrinsic absorptivity.

$1.5 \text{ J} < E_0 < 2.7$ J

The surface is cleaned in the laser spot, and a faint light is detected by eye. Probably, the vaporization of the surface defects occurs, with breakdown in the induced vapor, and superficial melting elsewhere. As predicted by the numerical code, α_t increases sharply from 0.04 to 0.075, as a result of the surface melting. For $E_0 > 1.8$ J, small craters appear, a small amount of heat is released by vaporization, and α_t bends down.

$2.7 \text{ J} < E_0 < 5$ J

A small, very luminous plasma appears on the surface (Fig. 6a). When E_0 grows, the craters become deep (Fig. 6b) and larger (Fig. 6c). The bulk vaporization threshold is reached for $E_0 = 2.7$ J, very close to the value given by the numerical code, i.e., $E_0 = 2.98$ J. Moverover, the code gives τ_v and, thus, upper bounds of the breakdown thresholds, $I_c = 5.3$ MW/cm^2, $F_c = 75$ J/cm^2. A maximum of α_t occurs at $E_0 = 2.7$ J, then α_t decreases as $(\tau_v - \tau_{fl})$ decreases (Fig. 4).

$5 \text{ J} < E_0 < 8$J

The crater covers the whole spot area, Fig. 7a, and the plasma jet extends sharply (Fig. 7b), taking the shape of an underexpanded supersonic jet with size independent of E_0. The plasma radiation is intense, as shown by the size effect, Fig. 5, and α_t rises from 0.064 to 0.145. In this energy range, α_v, evaluated with the hypothesis $m_f = 0$, rises to the maximal value 0.32.

$8 \text{ J} < E_0 < 10$ J

The heat coupled to the target comes primarily from the absorption of the uv plasma radiation and induces an additional vaporization; thus α_t decreases; α_v decreases a little, less than α_t. Other experiments, at $E_0 > 10$ J, should be necessary as confirmation.

V. Conclusion

These experiments on duraluminum in vacuum show that the maximal value of α_v, 0.32, found at the strong breakdown threshold, is roughly equal to the maximal value of α_t, 0.35, found at $p_0 = 760$ Torr, at the LSC-wave threshold, for a small value of the spot area/target area ratio.[2] Thus, the vapor plasma in vacuum radiates, in intensity and wavelength range, approximately as an air LSC-wave plasma. Additional experiments should be necessary to confirm this assertion. Moreover,

1) The bulk vaporization is a necessary condition in order to obtain a strong breakdown. The breakdown intensity threshold is as low in vacuum as at $p_0 = 760$ Torr, about 5 MW/cm^2.

2) The weak breakdown coming from the surface defect vaporization does not modify α_t and α_v.

3) Deep craters appear in isolated sites, probably surface defects, producing high local overintensities, local melting, then bulk vaporization due to the strong absorptivity increase during the melting.

4) At low intensity, the increase of α_t is due to the sharp variation of the infrared intensity during the melting. At high intensity, when the breakdown occurs, the strong absorption of the uv radiation by the metal induces further increases of α_t and α_v.

Acknowledgments

This work was supported by Direction des Recherches et Etudes Techniques, Ministry of Defense (DRET).

References

[1]Weyl, G., Pirri, A., and Root, R., "Laser Ignition of Plasma off Aluminum Surfaces," AIAA Paper 80-1319, July 1980.

[2]Marcus, S., Lowder, J. E., and Mooney, D L., "Large Spot Thermal Coupling of CO_2 Laser Radiation to Metallic Surfaces," *Journal of Applied Physics*, Vol. 47, July 1976, pp. 2966-2968.

[3]Ageev, V. P. et al., "Heating of Metals by CO_2 Laser Radiation Pulses," *Soviet Journal of Quantum Electronics*, Vol. 9, No. 1, Jan. 1979, p. 43.

[4]McKay, J. A. and Schriempf, J. T., "Anomalous Infrared Absorptance of Aluminum under Pulsed 10.6 μm Laser Irradiation in Vacuum," *Applied Physics Letters*, Vol. 35, No. 6, Sept. 15, 1979, p. 433.

[5]Glickler, S. L., Shraiman, B. J., Woodroffe, J. A., and Smith, M. J., "Thermally Insulated Defect Model for Plasma Initiation," AIAA Paper 80-1320, July 1980.

[6]Stern, G., Private Communication, Institute Franco-Allemand, Saint-Louis, France.

[7]McKay, J. A., Schriempf, J. T., Woodroffe, J. A., Cronburg, T. L., "Enhanced Laser-Metal Thermal Coupling in Vacuum," AIAA Paper 81-1152, June 1981.